Theoretical study of the interaction d^{10}–s^2 between Pt(0) and metals on the $[Pt(PH_3)_3M]$ complexes (M = Hg(0), Au(-I))

Fernando Mendizabal [a,*], Daniela Donoso [a], Claudio Olea-Azar [b], Raúl Mera [b]

[a] *Departamento de Química, Facultad de Ciencias, Universidad de Chile, Casilla 653, Santiago, Chile*
[b] *Departamento de Química Inorgánica y Analítica, Facultad de Ciencias Químicas y Farmacéuticas, Universidad de Chile, Casilla 233, Santiago 1, Chile*

Abstract

We studied the attraction between $[Pt(PH_3)_3]$ and the metals (Hg(0) and Au(-I)) in the hypothetical $[Pt(PH_3)_3M]$ isoelectronic complexes using ab initio methodology. We found that the changes around the equilibrium distance Pt–M and in the interaction energies are sensitive to the electron correlation potential. This effect was evaluated using several levels of theory, including HF, MPn ($n = 2$–4), CCSD and CCSD(T). In the $[Pt(PH_3)_3Hg]$ complex, at the different methodology levels are obtained interaction energies at the equilibrium distance R_e (Pt–Hg) range from 10 to 42 kJ/mol. Such magnitude are in the order of a metallophilic interaction. On the other hand, in the $[Pt(PH_3)_3Au]^-$ complex, the interaction energies Au–Pt are range from 35 to 129 kJ/mol, beyond the metallophilic interaction. At long-distances, the behaviour of the $[Pt(PH_3)_3$–M] interaction may be related mainly to electrostatic, charge-induced dipole and dispersion terms, involving the individual properties of $[Pt(PH_3)_3]$ and the individual metals. The dispersion term (R^{-6}) is found as the principal contribution in the stability at the long and short distances in the $[Pt(PH_3)_3Hg]$ complex. While in $[Pt(PH_3)_3Au]^-$ complex, the electrostatic and charge-induced dipole terms are found as the principal contributions in the stability at the long distances.

Keywords: Metallophilic attraction; Electron correlation effects; Pseudopotentials

1. Introduction

Closed-shell interactions range from extremely weak van der Waals forces to metallophilic and extremely strong d^{10}–s^2 or s^2–s^2 interactions [1,2]. It is found reports of systems with d^{10}–s^2 strong closed-shell interactions such as $AuHg^+$, $AuXe^+$ and $[Pt(PH_3)_3$–$Tl]^+$ with interaction energies of 179, 127 and 205 kJ/mol at CCSD(T) levels, respectively [3–6]. In these systems, two complementary forces have been identified: charge-induced dipole (cid) and dispersion (disp) interactions [7,8]. The largest contribution to the total energy is due to the charge-induced dipole interaction term, nevertheless the dispersion effects acquire significance near the equilibrium bond lengths. This is obtained when some from the subsystems presents an electronic configuration of the type s^2 and a formal charge.

On the other hand, one could think about a closed-shell hypothetical complex between $[Pt(PH_3)_3]$ and a transition metal $d^{10}s^2$ (M = Hg(O), Au(-I)) with the objective that in such systems prevail the forces of electrostatic, charge-induced dipole and dispersion as an interaction of the type van der Waals. The $[Pt(PH_3)_3Hg]$ and $[Pt(PH_3)_3Au]^-$ complexes are isoelectronic at the experimental $[Pt(PR_3)_3Tl]^+$ complex. The formation of stable adducts through metallophilic bonding of $d^{10}s^2$ ions to palladium(0) and platinum(0) has grown in the last years [9,10]. Hg(0) is often found as part of an electron-rich transition metal cluster or the face of *triangulo* clusters [11–13]. For example, in

* Corresponding author. Tel.: +56 2 9787397; fax: +56 2 2713888.
E-mail addresses: hagua@uchile.cl (F. Mendizabal), colea@uchile.cl (C. Olea-Azar).

the literature are found systems of the type $[Pt_3(\mu\text{-CO})(\mu\text{-dppm})_3\text{- Hg(0)}]^{2+}$ and $[Pt_3(\mu\text{-CO})(PPhPr_2)_3\text{–Hg(0)}]$.

The aim of the present work is to study theoretically the intermolecular interaction d^{10}–s^2 using the $[Pt(PH_3)_3M]$ (M = Hg(O), Au(-I)) isolectronic complexes as a model, comparing the Pt–M distances and estimating the strength of this interaction at the HF, MP2, MP3, MP4, CCSD and CCSD(T) levels by means of used scalar relativistic pseudopotentials (PPs). We report the structures and stability of these compounds and predict the most promising targets for synthetic work. In addition, in order to estimate the nature of the intermolecular interactions, we have included three simple expressions: electrostatic, charge-induced dipole and dispersion, calculated from the individual properties of $[Pt(PH_3)_3]$ and the metals (Hg(0), Au(-I)) at MP2 level [7,8].

2. Models and computational details

The models with the general formula $[Pt(PH_3)_3M]$ are depicted in Fig. 1. The models assume a C_{3v} point symmetry. The calculations were done using Gaussian 98 [14]. For the heavy elements Pt, Au and Hg, we used the Stuttgart pseudopotentials (PP): 18 valence-electron (VE) for Pt, 19-VE for Au and 20-VE for Hg [15]. Two f-type polarization functions were added to Pt ($\alpha_f = 0.70,0.14$) [16], Au ($\alpha_f = 0.20,1.19$) [17] and Hg ($\alpha_f = 0.50,1.50$) [18]. Also, the P atom was treated with PP, using double-zeta basis set and adding one d-type polarization function [19]. For hydrogen a valence-double-zeta basis set with p-polarization functions was used [20].

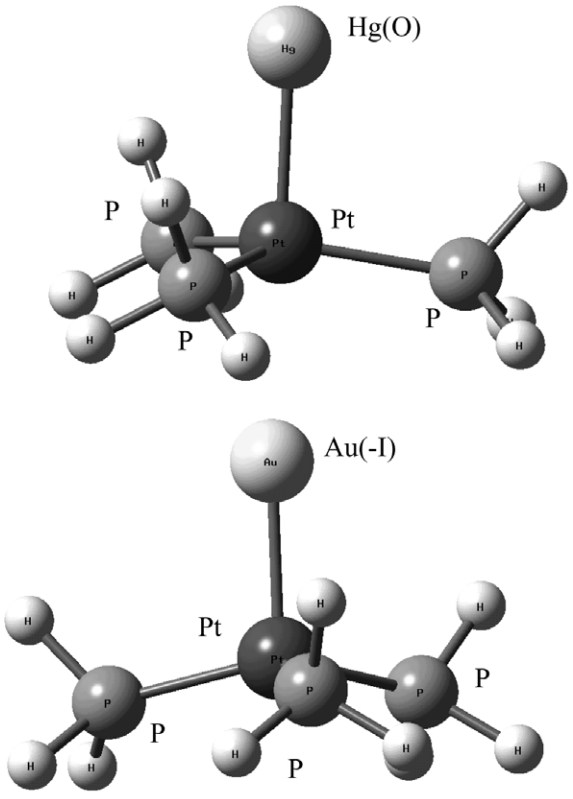

Fig. 1. The intermolecular interaction models of $[Pt(PH_3)_3Hg]$ and $[Pt(PH_3)_3Au]^-$.

The Pt–M intermolecular interaction energy was obtained using each of the following methods: HF, MP2–MP4, CCSD and CCSD(T). Though the computational methodologies do not consider spin-orbit interactions, the complex under investigation is a closed-shell singlet; hereby they should have only a minor importance.

The counterpoise correction for the basis-set superposition error (BSSE) was used for the interaction energies calculated. We have fully optimized the geometry of the model for each one of the methods mentioned above. Although, it is known that the MP2 approximation exaggerates the attractive interactions, this method gives a good indication of the existence of some type of interaction [21,22].

3. Results and discussion

Table 1 summarizes the principal geometric parameters obtained for the optimized geometries. We have included the $[Pt(PH_3)_3Tl]^+$ complex studied previously [6] with the intention of comparing the results obtained here. The interaction energies and the force constants Pt–M obtained in several theoretical levels are shown in Table 2. In this section, we will discuss about the geometries and the energies of interaction Pt···M in the complexes. The natural bond orbital (NBO) analysis is given in Tables 3 and 4. Finally, the origin of the intermolecular interactions will be studied as simple electrostatic, inductive and dispersion expressions obtained for the individual properties of the platinum complex and the metals (Hg(O), Au(-I)) (Table 5).

3.1. Short-distance behaviour

The results of our calculations (see Table 1) supports the original idea proposed that the $[Pt(PH_3)_3M]$ systems show a closed-shell interactions of type van der Waals. Concerning the Pt–M distances and the interaction energies (see Table 2), it is clear that the electronic correlation effects play an important role in the stability of systems. The Pt–M distances obtained with all methods show oscillations; however, the distances obtained with the MP2 and MP4 methods are the shortest. It is worth noting that the MP2 approximation overestimates the metallic interactions [21,22]. The distances obtained in this work indicates that the Pt···M (M = Hg(0), Au(-I)) contact is a strong closed-shell interaction, which goes beyond the classic metallophilic interaction [23,24]. The Pt–M force constants (F) calculated in the complexes (also shown in Table 2) are indicative of a weak interaction, due to the heavy metals nature of the involved centers.

Other manifestation of the interaction in the complexes is the angle PPtM°. Such angle shows a deviation compared to the $[Pt(PH_3)_3]$ free from 90° to 97.6° in $[Pt(PH_3)_3Hg]$ (MP2) and 101.3° $[Pt(PH_3)_3Au]^-$ (MP2). There is a change in the rehybridization of the platinum

Table 1
Main geometric parameters of the model studied $[Pt(PH_3)_3M]$ (M = Hg(0), Au(-I), Tl(+I))

System	Method	Pt–M	Pt–P	P–H	P–Pt–M°	P–Pt–P°	H–P–Pt°
$[Pt(PH_3)_3Hg]$	MP2	270.6	229.2	142.5	97.68	118.24	120.83
	MP3	300.7	234.1	142.5	94.75	119.32	121.07
	MP4	270.3	233.6	143.0	98.28	117.96	120.84
	CCSD	302.0	233.9	142.8	97.68	118.24	120.83
	CCSD(T)	297.5	233.7	142.9	98.30	118.35	120.86
$[Pt(PH_3)_3Au]^-$	HF	325.8	235.5	142.1	95.89	118.96	121.14
	MP2	261.8	226.7	143.6	101.33	119.98	122.37
	MP3	286.5	232.0	143.2	98.18	118.01	122.22
	MP4	260.9	231.4	144.2	102.79	118.24	122.43
	CCSD	282.2	231.9	143.4	100.54	118.45	122.17
	CCSD(T)	280.2	231.6	143.6	101.68	118.16	122.25
$[Pt(PH_3)_3Tl]^+$ [6]	HF	279.9	242.9	141.1	90.0	120.0	119.2
	MP2	266.9	233.6	141.9	90.0	120.0	119.4
	MP3	281.3	236.4	141.5	90.0	120.0	120.4
	MP4	275.7	235.2	141.2	90.0	120.0	119.7
	CCSD	279.2	235.7	141.6	90.0	120.0	120.3
	CCSD(T)	277.3	234.6	141.6	90.0	120.0	119.9
$[Pt(PPhpy)_3Tl](NO_3)$	Exp.[3]	289.9	228.6		92.0	119.9	
$[Pt(PPhpy)_3Tl](CH_3CO_2)$	Exp.[3]	286.6	227.6		92.7	119.8	

Distances in pm and angles in degrees.

Table 2
Optimized Pt–M (M = Hg(0), Au(-I)) distance (R_e), in pm

System	Method	Pt–M	ΔE	F
$[Pt(PH_3)_3Hg]$	HF	276.8	+15.7	–
	MP2	276.8	−42.2	12.7
	MP3	300.7	−10.3	1.7
	MP4	270.3	−36.9	8.0
	CCSD	302.0	−18.8	4.5
	CCSD(T)	297.5	−23.0	5.5
$[Pt(PH_3)_3Au]^-$	HF	325.8	+8.6	–
	MP2	261.8	−121.9	27.4
	MP3	286.5	−35.6	9.9
	MP4	260.9	−129.3	27.6
	CCSD	282.2	−52.5	11.5
	CCSD(T)	280.2	−65.6	13.6
$[Pt(PH_3)_3Tl]^+$ [6]	HF	279.9	−134.1	66.1
	MP2	266.9	−202.6	125.1
	MP3	281.3	−136.1	66.4
	MP4	275.6	−205.5	92.7
	CCSD	279.2	−171.6	82.7
	CCSD(T)	277.3	−203.6	97.1

Interaction energies (ΔE), with counterpoise correction, in kJ/mol. Force constant (F) Pt–M, in N m^{-1}.

Table 3
NBO analysis of the MP2 density for $[Pt(PH_3)_3Hg]$, $[Pt(PH_3)_3]$ and Hg(0)

System	Atom	Natural	Natural electron configuration
$[Pt(PH_3)_3Hg]$	Hg	0.0551	$5d^{10.0}\ 6s^{1.94}\ 7p^{0.01}$
	Pt	−0.2864	$5d^{9.65}\ 6s^{0.55}\ 6p^{0.05}\ 5f^{0.01}\ 6d^{0.02}\ 7p^{0.01}$
	P	0.1723	$3s^{1.43}\ 3p^{3.32}\ 3d^{0.04}\ 4s^{0.01}\ 4p^{0.03}$
	H	−0.0317	$1s^{1.03}$
$[Pt(PH_3)_3]$	Pt	−0.2864	$5d^{9.64}\ 6s^{0.52}\ 6p^{0.03}\ 6d^{0.01}\ 7p^{0.01}$
	P	0.1723	$3s^{1.44}\ 3p^{3.30}\ 3d^{0.04}\ 4s^{0.01}\ 4p^{0.03}$
	H	−0.0355	$1s^{1.03}$
Hg(0)	Hg	0.0000	$5d^{10.0}\ 6s^{2.00}\ 6p^{0.00}$

Table 4
NBO analysis of the MP2 density for $[Pt(PH_3)_3Au]^-$, $[Pt(PH_3)_3]$ and Au(-I)

System	Atom	Natural	Natural electron configuration
$[Pt(PH_3)_3Au]^-$	Au	−0.8988	$5d^{9.80}\ 6s^{1.85}\ 6p^{0.08}\ 5f^{0.10}\ 6d^{0.06}\ 7p^{0.01}$
	Pt	−0.2176	$5d^{9.26}\ 6s^{0.60}\ 6p^{0.11}\ 7s^{0.01}\ 5f^{0.11}\ 6d^{0.11}\ 7p^{0.02}$
	P	0.1199	$3s^{1.43}\ 3p^{3.33}\ 3d^{0.08}\ 4p^{0.05}$
	H	−0.0315	$1s^{1.02}\ 2s^{0.01}\ 2p^{0.01}$
$[Pt(PH_3)_3]$	Pt	−0.2425	$5d^{9.32}\ 6s^{0.64}\ 6p^{0.07}\ 7s^{0.01}\ 5f^{0.10}\ 6d^{0.10}\ 7p^{0.01}$
	P	0.1067	$3s^{1.42}\ 3p^{3.35}\ 3d^{0.08}\ 4s^{0.01}\ 4p^{0.04}$
	H	−0.0086	$1s^{1.00}\ 2s^{0.01}\ 2p^{0.01}$
Au(-I)	Au	−1.0000	$5d^{10.0}\ 6s^{2.00}\ 6p^{0.00}$

atom from sp^2 toward sp^3 resulting in a partial pyramidalization. Comparing these results with the $[Pt(PH_3)_3Tl]^+$ complex at theoretical and experimental levels the greater difference corresponds to the lost of plane of the platinum. This structural change produces a dipole moment different of zero for such fragment of platinum.

The magnitude of the interaction energies obtained varies according to the method used between 42.2 kJ/mol (MP2) and 23.0 kJ/mol (CCSD(T)) in $[Pt(PH_3)_3Hg]$, and 121.9 kJ/mol (MP2) and 65.6 kJ/mol in $[Pt(PH_3)_3Au]^-$. At level HF, the complexes do not show stable interaction energies. For the $[Pt(PH_3)_3Hg]$ complex, the magnitude of energies are associated with weak metallophilic interactions. On the other hand, in the $[Pt(PH_3)_3Au]^-$ complex the interaction energies are more near to a formal bond Pt–Au. For this last system, this might be indicative of an orbital stabilization due to the formation of stable adducts between the fragment of platinum and the gold anion. The $[Pt(PH_3)_3Tl]^+$

Table 5
Finite field calculations (a.u.) of electric properties of $[Pt(PH_3)_3]$, Hg(0) and Au(-I) at MP2 level

Properties	$[Pt(PH_3)_3]$[a]	$[Pt(PH_3)_3]$[b]	Hg(0)	Au(-I)
Dipole moment (μ)	0.7434	0.8012	0.0	0.0
Polarizability (α)	124.59	124.97	27.56	46.62
$\alpha_{\parallel}-\alpha_{\perp}$	52.66	53.29	0.0	0.0
Quadrupole moment (Θ)	6.375	3.094	0.0	0.0
First ionization potential (IP_1)	0.2750	0.2785	0.3268	0.0423

[a] Geometry from $[Pt(PH_3)_3Hg]$ complex.
[b] Geometry from $[Pt(PH_3)_3Au]^-$ complex.

complex shows interaction energies larger than the previous complexes due to that the terms of charge-induced dipole and dispersion terms are added.

To obtain a better insight on such stabilization, we have depicted in Figs. 2 and 3 an interaction diagram for the frontier molecular orbitals of both fragments $[Pt(PH_3)_3]$ and the metals (Hg(0) and Au(-I)). In the figures, the left and right side of the correspond to the frontier levels of the platinum complex and a free metal, respectively. The center of the diagram corresponds to the molecular orbitals for the $[Pt(PH_3)_3$–M] complexes. Two orbital show a strong interaction: $31a_1$ and $26a_1$ in $[Pt(PH_3)_3Hg]$ and $31a_1$ and $28a_1$ in $[Pt(PH_3)_3Au]^-$, whereas the molecular orbitals remain without changes (except the LUMO levels). Both group of orbitals generate the bonding ($26a_1$ and $28a_1$) and antibonding ($31a_1$) sigma levels from dz^2 (Pt) and $6s^2$ (Au and Hg), respectively. These two molecular orbitals are doubly occupied. These results clearly indicated a net effect of no bonding through the orbital interactions.

The natural bond orbital (NBO) [25] population analysis for the complexes are shown in Tables 3 and 4. This analysis is based on the MP2 density. From the Table 3, it is possible to observe a charge transfer from the Hg toward the $[Pt(PH_3)_3]$ fragment (0.0551e) in the $[Pt(PH_3)_3$–Hg] complex. While in Table 4 is observed a small charge transfer from the Au(-I) toward $[Pt(PH_3)_3]$ (−0.1012e). The platinum shows no variability in its charge. The gross population per atom shell shows that for the 6p orbital of metals (Hg and Au) are almost thoroughly occupation. The charge of the 6s orbital, on the contrary does not change maintaining its inert character.

3.2. Long-distance behaviour

The MP2 results for the long-distance attraction between $[Pt(PH_3)_3]$ and M (Hg(0) and Au(-I)) are shown in Figs. 4 and 5. Energy minima occur at R_e (see Table 2). At the equilibrium distance R_e (Pt–M), the differences in energy between MP2 and second order contribution ($E(2)$) of electronic correlation corresponds to the Hartree–Fock term. At long-range distances, the $[Pt(PH_3)_3Hg]$ complex shows that the $E(2)$ term behaves as R^{-6} (Pt–Hg) and agrees with the dispersion formula used the Eq. (1). While in the $[Pt(PH_3)_3Au]^-$ system can be noticed that the HF level is prevailing at large Pt–Au distance. We have used the Eq. (2), to describe the terms involved in the limit of large distances for the last complex. That equation includes the electrostatic (elect), charge-induced dipole (cid) and the dispersion (disp) terms, which can be used to understand the predominant mechanism of bonding.

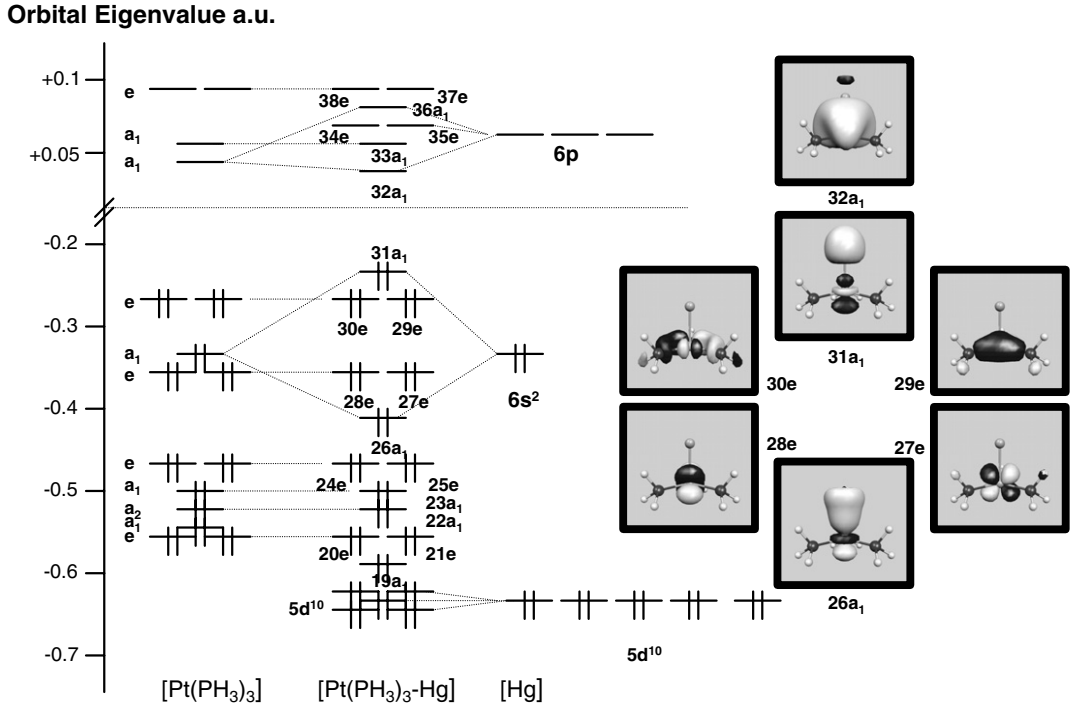

Fig. 2. Interaction diagram obtained for the frontier molecular orbitals for $[Pt(PH_3)_3]$ and Hg fragments.

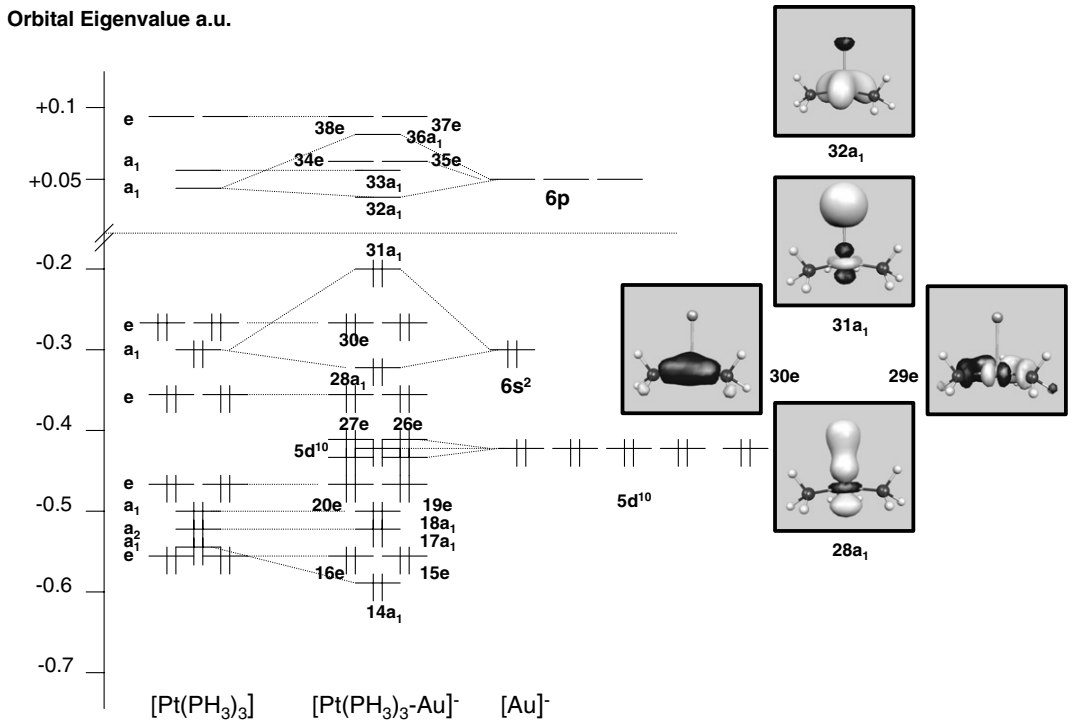

Fig. 3. Interaction diagram obtained for the frontier molecular orbitals for $[Pt(PH_3)_3]$ and Au^- fragments.

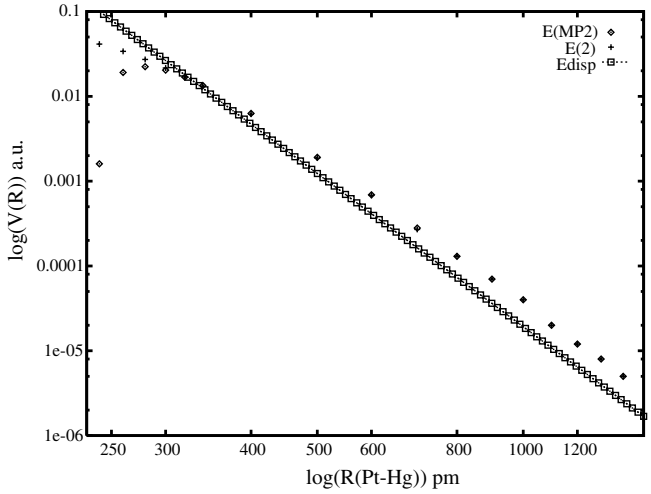

Fig. 4. Long distance interaction energies of the model at the MP2 level by $[Pt(PH_3)_3$-Hg] complex.

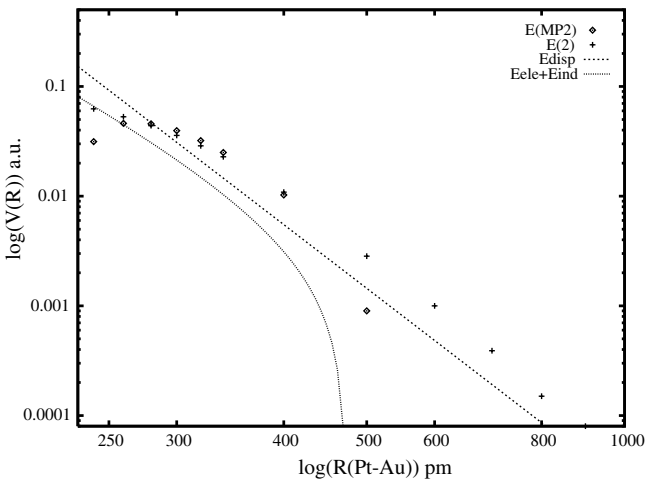

Fig. 5. Long distance interaction energies of the model at the MP2 level by $[Pt(PH_3)_3$–Au(-I)] complex.

$$E = \mathrm{Edisp} \cong -3/2\frac{\alpha^{\mathrm{Pt}}\alpha^{\mathrm{Hg}}}{R^6}\left[\frac{\mathrm{IP}^{\mathrm{Pt}}\mathrm{IP}^{\mathrm{Hg}}}{\mathrm{IP}^{\mathrm{Pt}}+\mathrm{IP}^{\mathrm{Hg}}}\right] \quad (1)$$

$$E = \mathrm{Eelect} + \mathrm{Ecid} + \mathrm{Edisp} \cong \left[\frac{\mu^{\mathrm{Pt}}}{R^2}+\frac{\Theta^{\mathrm{Pt}}}{R^3}\right] - 1/2\frac{1}{R^4}\left[\alpha^{\mathrm{Pt}} + 3/2(\alpha_{\|}-\alpha_{\perp})^{\mathrm{Pt}}\right] - 3/2\frac{\alpha^{\mathrm{Pt}}\alpha^{\mathrm{Au}}}{R^6}\left[\frac{\mathrm{IP}^{\mathrm{Pt}}\mathrm{IP}^{\mathrm{Au}}}{\mathrm{IP}^{\mathrm{Pt}}+\mathrm{IP}^{\mathrm{Au}}}\right] \quad (2)$$

Table 5 lists the dipolar moments, static polarizabilities, quadrupole moments and ionization potentials (IP) used for $[Pt(PH_3)_3]$, Hg(0) and Au(-I) obtained at the MP2 level. For the case of the $[Pt(PH_3)_3Hg]$ system describes a behaviour of a metallophilic interaction dominated by the dispersion term at short and long distances Pt–Hg. However, in $[Pt(PH_3)_3Au]^-$ due to the negative charge of system and the distorted geometry of the platinum fragment, permit that at long distance Pt–Au the interaction energy is dominated by the electrostatic and induction terms. Both terms at short distance tend to be cancelled mutually due to that have opposite signs. This is an important difference to the isoelectronic $[Pt(PH_3)_3$–$Tl]^+$ complex [6].

This last specie showed a dispersion interaction and long-range polarization effects. The leading attractive term in the potential comes from the polarization that $[Pt(PH_3)_3]$ undergoes by Tl^+. Thus, the largest contribution to the

total energy is due to the charge-induced dipole interaction term, nevertheless the dispersion effects acquire significance near the equilibrium bond lengths. It showed an R^{-4} behaviour at large distances.

4. Conclusions

The existence of the $[Pt(PH_3)_3Hg]$ and $[Pt(PH_3)_3Au]^-$ complexes has been predicted. These complexes have a structure analogous to the corresponding $[Pt(PH_3)_3–Tl]^+$. To difference of the $[Pt(PH_3)_3–Tl]^+$ complex, the studied systems here describe a different behaviour. The $[Pt(PH_3)_3Hg]$ complex shows a metallophilic interaction. The dispersion term (R^{-6}) is found as the principal contribution in the stability at the long and short distances. While the $[Pt(PH_3)_3Au]^-$ complex describes a strong metallophilic interaction. At long-distances, the electrostatic and charge-induced dipole terms are found as the principal contributions in the stability for such specie. The frontier orbital analysis confirmed that a formal bond through an orbital interaction does not exist.

Acknowledgements

This investigation was financed by FONDECYT N° 1060044 (Conicyt-Chile) and MIDEPLAN through Millennium *Nucleus for Applied Quantum Mechanics and Computational Chemistry* P02-004-F.

References

[1] P. Pyykkö, Chem. Rev. 97 (1997) 597.
[2] F. Luo, G.C. Mcbane, G.-S. Kim, C.F. Giese, W.R. Gentry, J. Chem. Phys. 98 (1993) 3564.
[3] V.J. Catalano, B.L. Bennett, S. Muratidis, B.C. Noll, J. Am. Chem. Soc. 123 (2001) 173.
[4] R. Wesendrup, P. Schwerdtfeger, Angew. Chem. Int. Ed. 39 (2000) 907.
[5] D. Schröder, H. Schwarz, J. Hrusák, P. Pyykkö, Inorg. Chem. 37 (1998) 624.
[6] F. Mendizabal, G. Zapata-Torres, C. Olea-Azar, Chem. Phys. Letters. 412 (2005) 477.
[7] R. Wesendrup, P. Schwerdtfeger, Angew. Chem. Int. Ed. 39 (2000) 907.
[8] J.P. Read, A.D. Buckingham, J. Am. Chem. Soc. 119 (1997) 9010.
[9] L.H. Gade, Angew. Chem. Int. Ed. 40 (2001) 3573.
[10] L.H. Gade, Angew. Chem. Int. Ed. 32 (1993) 24.
[11] G. Schoettel, J.J. Vittal, R.J. Puddephatt, J. Am. Chem. Soc. 112 (1996) 6400.
[12] A.D. Burrows, D.M. Mingos, Coord. Chem. Rev. 154 (1996) 19.
[13] D. Imhof, L.M. Venanzi, Chem. soc. Rev. (1994) 185.
[14] M.J. Frisch, G.W. Trucks, H.B. Schlegel, P.M.W. Gill, B.G. Johnson, M.A. Robb, J.R. Cheeseman, K.T. Keith, G.A. Petersson, J.A. Montgomery, K. Raghavachari, M.A. Al-Laham, V.G. Zakrzewski, J.V. Ortiz, J.B. Foresman, J. Cioslowski, B.B. Stefanov, A. Nanayakkara, M. Challacombe, C.Y. Peng, P.Y. Ayala, W. Chen, M.W. Wong, J.L. Andres, E.S. Replogle, R. Gomperts, R.L. Martin, D.J. Fox, J.S. Binkley, D.J. Defrees, J. Baker, J.P. Stewart, M. Head-Gordon, C. Gonzalez, J.A. Pople, Gaussian 98, Inc., Pittsburgh PA, 2002.
[15] D. Andrae, U. Haeussermann, M. Dolg, H. Stoll, H. Preuss, Theor. Chim. Acta 77 (1990) 12.
[16] M. Dolg, P. Pyykkö, N. Runeberg, Inorg. Chem. 34 (1996) 7450.
[17] P. Pyykkö, N. Runeberg, F. Mendizabal, Chem. Eur. J. 3 (1997) 1451.
[18] P. Pyykkö, M. Straka, T. Tamm, Phys. Chem. Chem. Phys. 1 (1999) 3441.
[19] A. Bergner, M. Dolg, W. Küchle, H. Stoll, H. Preuss, Mol. Phys. 80 (1993) 1431.
[20] S. Huzinaga, J. Chem. Phys. 42 (1965) 1293.
[21] P. Pyykkö, F. Mendizabal, Inorg. Chem. 37 (1998) 3018.
[22] F. Mendizabal, G. Zapata-Torres, C. Olea-Azar, Chem. Phys. Lett. 382 (2003) 92.
[23] P. Pyykkö, Angew. Chem. Int. Ed. 43 (2004) 4412.
[24] P. Pyykkö, F. Mendizabal, Chem. Eur. J. 3 (1997) 1458.
[25] J.E. Carpenter, F. Weinhold, J. Mol. Struct. 169 (1988) 41.